Expanding the bandwidth of planar MNG materials with co-directional split-ring resonators*

Tang Ming-Chun(唐明春), Xiao Shao-Qiu(肖绍球)†, Wang Duo(王 多), Ge Guang-Ding(葛广顶), Bai Yan-Ying(柏艳英), Zhang Jun-Rui(张俊睿), and Wang Bing-Zhong (王秉中)

Institute of Applied Physics, University of Electronic Science and Technology of China, Chengdu 610054, *China*

(Received 29 November 2010; revised manuscript received 28 December 2010)

An effective approach to expand the bandwidth of negative permeability of small-sized planar materials is proposed. Based on qualitative analysis of equivalent circuit models, the fractional bandwidth of an μ-negative (MNG) material is expanded from 3.53% up to 12.87% by adding split-ring resonators (SRRs) and arranging them by proposed steps. Moreover, the experimental results validate the effectiveness of bandwidth-expanding methods, which is promising for the extensive application of metamaterials in the microwave field.

Keywords: planar μ-negative materials, bandwidth expanding, co-directional split-ring resonators

PACS: 78.67.Pt, 73.20.Mf **DOI:** 10.1088/1674-1056/20/6/067805

1. Introduction

Metamaterials are artificial materials that show negative permittivity and/or negative permeability over a limited frequency bandwidth.[1−8] Since negative permittivity occurs naturally in metals, as described by the Drude electron model in metals,[9] ε-negative (ENG) materials are easy to realize. However, the acquisition of negative permeability is a real challenge since there are no free magnetic charges in nature.[1,10] Even so, resonator structures such as split-ring resonators (SRRs),[10] spiral resonators (SRs),[11] S-shaped resonators,[12] Ω-shaped resonators,[13] U-shaped resonators,[14] single loop resonators,[15] and micro-split SRRs[16] have been proven to have negative permeability in certain frequency ranges. Unfortunately, one main obstacle for the practical application of these MNG materials lies in the limitation that the bandwidth they demonstrated is quite narrow. In order to overcome the bandwidth limit, two methods have been presented. One method managed to fabricate all-dielectric MNG material[17] with an array of high dielectric constant cylinders. In the other effective method, Rudolph and Gribic recently reported a volumetric negative-refractive-index material consisting of a periodic cage of backward-wave transmission lines.[18,19] However, the above approaches have some deficiencies: in the all-dielectric metamaterial method, the permittivity and the loss of the photonic crystal are too high; and in the fabrication of volumetric metamaterial, the difficulty of the method makes it very expensive. As an alternative approach, a novel method of expanding the bands of MNG materials is proposed. In this paper, several planar evolved co-directional SRRs are overlappingly placed to compound a broadband MNG material. Interestingly, without resorting to high dielectric constant cylinders[17] or a three-dimensional transmission-line "cage",[18,19] the planar co-directional SRR structure is quite compatible with standard printed-circuit-board (PCB) fabrication techniques, which avoids additional high loss from ceramics with high permittivity, dramatically reduces the complexity of manufacturing process and reasonably accomplishes the mechanical stability of the MNG material's structure.

2. Planar evolved SRR fabrication

In 1999, Pendry *et al.*[10] first proposed a double split ring resonator (SRR) medium to design a material with negative permeability.[10] Since then, Zharov *et al.*[20] introduced a typically simple single SRR geometry, which has magnetic resonance per-

*Project supported partially by the National Natural Science Foundation of China (Grant Nos. 60872034 and 60971029), the New-Century Talent Program of the Education Department of China (Grant No. NCET070154), the National Defense Research Funding (Grant No. ZJ10DZ02111), and the Hi-Tech Research and Development Program of China (Grant No. 2009AA01Z231).

†Corresponding author. E-mail: xiaoshaoqiu@uestc.edu.cn

© 2011 Chinese Physical Society and IOP Publishing Ltd

formance qualitatively similar to the double SRR in Ref. [10]. Here, we add two parallel arms to the single SRR to construct a single-sided planar-evolved SRR, as shown in Fig. 1(a). Here, we take simulations of the single-sided planar SRR with commercially available numerical electromagnetic solver HFSS[21] as follows. In the simulations, the scattering properties of the MNG material (including the reflection coefficient and transmission coefficient) are studied with a plane wave at normal incidence on the xy plane. The proper boundary conditions[22,23] are set to coincide with the electromagnetic environment in Fig. 1(a), i.e., perfectly electric conducting (PEC) and perfectly magnetic conducting (PMC) boundary conditions are imposed in x and y directions respectively and input/output ports are imposed in the z direction. In this case, a time-alternating magnetic field directed along the y axis will generate a magnetic response with circulating currents being induced in the ring, also schematically shown in Fig. 1(a). Thus, the proposed SRR can predominantly give a magnetic resonant response to the propagating electromagnetic field.[22] According to Refs. [20], [24], and [25], it behaves as an L–C resonator that can be excited by an external magnetic flux. We present its qualitative equivalent circuit in Fig. 1(b). It is seen that its magnetic resonance frequency can be adjusted by changing the L–C resonance circuit. It is interesting to note that we can easily adjust the lengths of the double parallel arms L (i.e., the equivalent capacitance C_0' and inductance) in order to obtain the required resonance frequency without changing other physical dimensions or destroying the overall size. Moreover, verified by our simulation, the additional arm has a negligible effect on the MNG bandwidth of SRR in Fig. 1. Owing to that particular characteristic, the proposed evolved SRR is quite suitable for broadband MNG material design (which will be studied in Section 3).

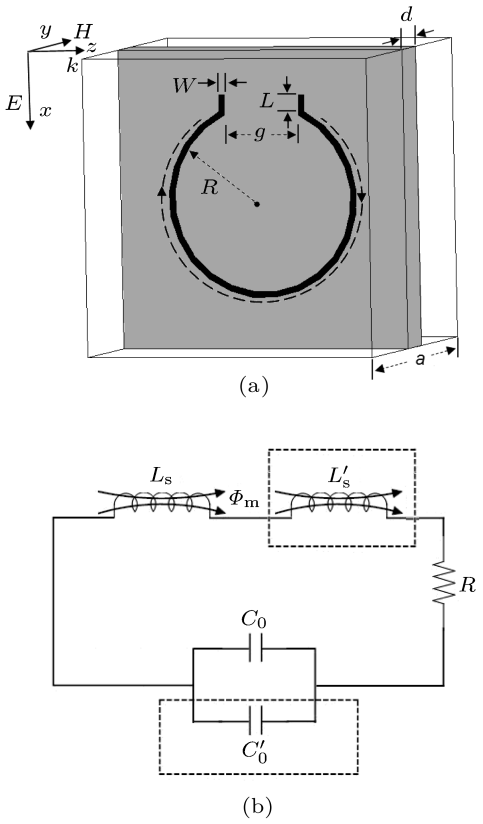


Fig. 1. Proposed single-sided planar evolved SRR. (a) Configuration of single-sided planar evolved SRR in a specific electromagnetic environment; $g = 2.6$ mm, $L = 0.6$ mm, $W = 0.2$ mm, $R = 3.1$ mm, the FR4 substrate thickness $d = 1.6$ mm with loss tangent 0.02 and the cubic length $a = 10$ mm. (b) Its qualitative equivalent circuit: L_s represents the total equivalent inductance, C_0 is the total equivalent capacitance of the proposed SRR in Fig. 1(a) without the parallel arms (they also represent the total equivalent inductance and capacitance for the SRR in Ref. [10], respectively), and the L_s' and C_0' (in the dotted areas) imply the additional equivalent inductance and capacitance of the double parallel arms, respectively.

Figure 2 shows the effect of the length L of the double parallel arms on the resonance frequency. It demonstrates that when the length L changes from 0.2 mm to 1.8 mm, the resonance dip drops from 5.04 GHz to 4.14 GHz accordingly, while the resonance strength and bandwidth remain almost unchanged. As for its equivalent circuit model in Fig. 1(b), the L_s' and C_0' increase simultaneously due to the increase of the arm's length L, thus its magnetic resonance frequency decreases, in agreement with the simulation results in Fig. 2. Then, in order to discuss its magnetic response characteristic, the corresponding effective permittivity and permeability are retrieved based on the magnitudes and phases of the scattering property,[26] shown in Figs. 3(a) and 3(b), respectively. It is seen that the permittivity remains positive in Fig. 3(a), while the permeability exhibits a negative value (with a narrow fractional bandwidth of about 3.53%) in Fig. 3(b) within each resonance frequency region in Fig. 2. Meanwhile, we notice some ripples in the curve of the effective electromagnetism parameters within the resonance frequency region. The reason is that the resonant behaviour of the effective permeability is accompanied by an antiresonant behaviour of the effective permittivity, which has been analysed in detail in Ref. [27].

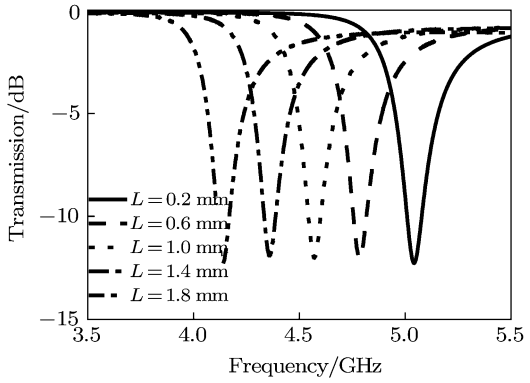


Fig. 2. Effect of the arm lengths L on transmission characteristics.

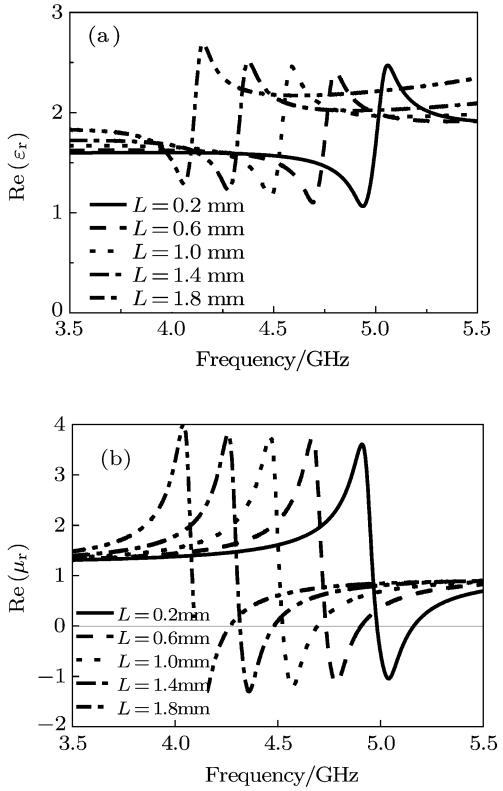


Fig. 3. The retrieved electromagnetism parameters. (a) Effective permittivity; (b) Effective permeability.

3. Expanding the MNG bandwidth by multiple co-directional SRRs

In order to improve the resonance strength and expand the resonance frequency bandwidth, we propose one effective evolution approach, which can be divided into the following three key steps. In the first step, another single SRR with the same gap-directions (along the $-x$ axis) and dimensions as the evolved SRR in Fig. 1(a) is mounted at the other side of the substrate to compound a pair-SRR. Figure 4 shows that the resonance strength is distinctly improved (in Fig. 4(a))[16,28] and the frequency bandwidth of negative permeability is also broadened[28] to 6.45% (in Fig. 4(b)) accordingly. The other two pair-SRRs are then added to make a triple-SRR structure. In this design, the triple pair-SRRs are superpositionally placed at a co-centre with co-directions. As mentioned in the first step, the SRRs in the middle pair have the same dimensions as the evolved SRR in Fig. 1(a). In this step, the pairs in the other two pairs take different sizes, as shown in Fig. 5(a).

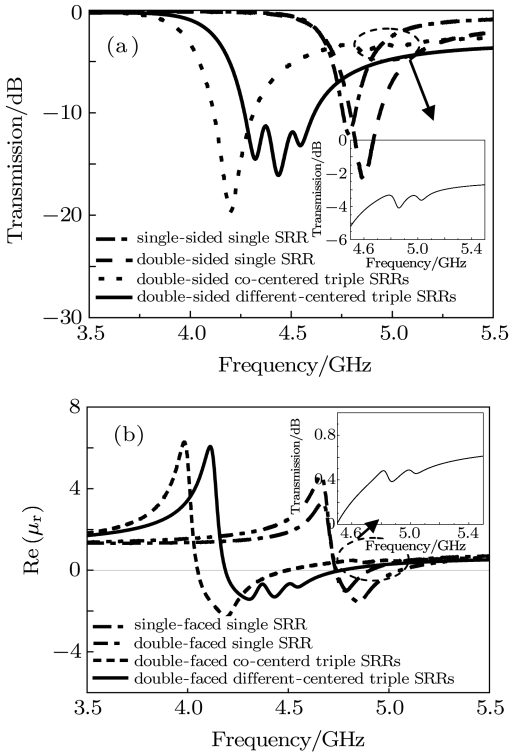


Fig. 4. Magnetic response of different type SRRs. (a) Transmission characteristic; (b) Real parts of effective permeability.

The aim of adding two pair-SRRs is to combine multiple adjacent resonance frequency regions into a wider MNG bandwidth. As in Fig. 1(a), the magnetic response is excited when the circulating currents are induced by an external magnetic field. Similarly, when a time-alternating external magnetic field is imposed, these three pair-SRRs can exhibit simultaneous magnetic responses, thus generating three adjacent resonance frequency regions. Since the current distribution in each SRR and the layout of the SRRs are similar, the mutual coupling between adjacent rings is much lower than the multi-split ring resonators in Refs. [23] and [29] or the SRRs with rotated inner rings in Ref. [30]. The reason for this has been analysed in

detail in Ref. [30] with the aid of an equivalent circuit for a double SRR with a rotated inner ring. Therefore, these three adjacent resonance frequency regions can be combined into a wider MNG bandwidth. The results in Fig. 4 validate that this approach can broaden the resonance frequency region (with MNG bandwidth 10.30%).

However, the resonances for the two upper frequencies are not strong enough to achieve negative permeability, labeled with the dotted circles in Fig. 4(b). Thus, in the third step, the strengths of two upper resonances should be improved to uniformize the resonance strength as a whole. In our numerical study of this type of SRR, it is found that the shorter distance between the gap of the inner ring and that of the outer ring in x axis is (i.e., the relative distances OO'' and OO', respectively), the stronger resonance the inner ring exhibits. Hence, by adjusting the distance between the gaps of the outer and inner SRRs (i.e., the relative positions of each centre along the x axis) in the x axis and the lengths of double parallel arms (the reason for this will be analysed in the next paragraph), the strengths can be uniformized well, and the design is shown in Fig. 5(a). Results from the third step are also given in Fig. 4 for comparison. It is seen that the strengths of the triple resonance frequencies are optimized to uniform successfully and the MNG bandwidth is broadened to 12.87%. It is worthwhile mentioning that if the number of SRRs is enlarged according to the evolution method based on the above analysis, the MNG bandwidth can be expected show further improvement.

The reason for adjusting the lengths of the parallel arms in the third step is also discussed, as follows. Figure 5(b) presents the equivalent circuit of triple pair-SRRs in Fig. 5(a). It is worthwhile mentioning that the mutual coupling (M_1, M_2, and M_3) can impact the resonance frequency of each ring slightly, even though it is very low in this design. Therefore, it is necessary to amend the resonance frequency based on the analysis in Fig. 5(b). As is mentioned in Fig. 2, the adjustment of lengths of the parallel arms of the inner and middle pair-SRRs (L and L') can alter each resonance frequency easily. Hence, we accommodate the lengths of double parallel arms (i.e., altering the additional inductances (L_1' and L_0') and capacitances (C_1' and C_0'), respectively) to offset the effect of M_1, M_2, and M_3, ensuring that the three resonance frequencies are close enough to each other to form a wider MNG bandwidth.

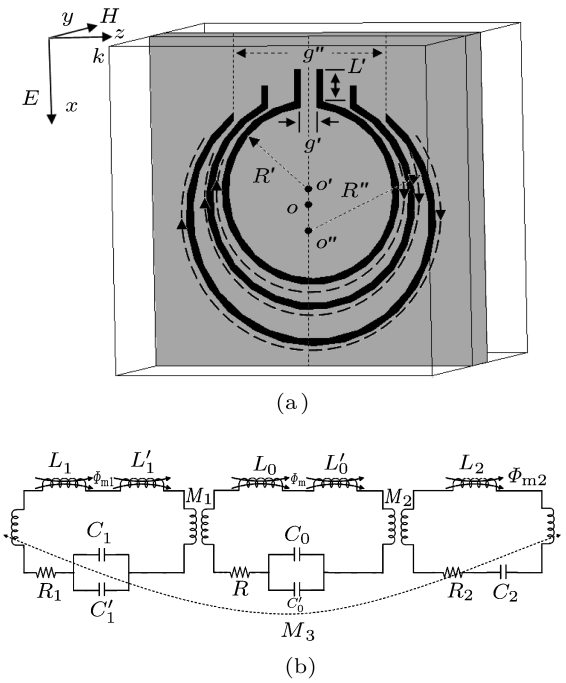


Fig. 5. Double-sided planar evolved co-directional SRRs. (a) The geometry: $g' = 0.5$ mm, $L' = 0.98$ mm, $R' = 2.6$ mm, $OO' = 0.25$ mm, $g'' = 4.8$ mm, $R'' = 3.75$ mm, $OO'' = 0.45$ mm. (b) Its qualitatively equivalent circuit (L_1, L_0 andL_2 indicate the equivalent inductances of the inner, middle and outer pair-SRRs, respectively. C_1, C_0, and C_2 represent the equivalent capacitances of the inner, middle and outer pair-SRRs, respectively, without the parallel arms; C_1' and C_0' imply the additional equivalent capacitance of the double parallel arms in the inner and middle pair-SRRs, respectively. L_1' and L_0' imply the additional equivalent inductances of the double parallel arms in the inner and middle pair-SRRs, respectively. M_1, M_2, and M_3 indicate the mutual inductance couplings between the inner and middle, middle and outer, inner and outer pair-SRRs, respectively).

Furthermore, its low mutual coupling characteristic is numerically discussed. Firstly, it is seen from Fig. 6(a) that when the gap of outer pair-SRR gap (g'') increases, its magnetic resonance frequency decreases, while the higher resonance frequencies, as well as their resonance strengths, for the other two pair-SRRs remain fixed on the whole especially for the inner pair-SRR exhibiting low mutual coupling.[30,31] When the length of the inner ring's arm pair (L') changes from zero to 0.58 mm, the corresponding magnetic resonance frequency decreases in Fig. 6(b), and the lower resonance frequencies as well as the resonance strengths, for the other two pair-SRRs, also remain fixed on the whole. It is noted that when the upper resonance frequency (for the inner pair-SRR) gets closer to the other resonance frequencies (i.e., its arm's length L' is larger than 0.58 mm here), the mutual

coupling effect becomes more significant and cannot be neglected. Therefore, we come to the conclusion that when the resonance frequencies between the inner and outer rings are not that close to each other, their mutual coupling is negligible. However, when their resonance frequencies are very closer to each other, the mutual coupling becomes more significant (M_1, M_2, and M_3). Since the resonance frequencies between the inner and outer pair-SRRs is further away than the other (i.e., the resonance frequencies between inner and middle, and outer and middle), the mutual coupling M_3 is smaller than M_1 and M_2. In order to fabricate a wideband MNG material unit, we compensate the mutual coupling by simply adjusting the two arms L and L' (i.e., altering the additional inductance and capacitance for each ring, respectively).

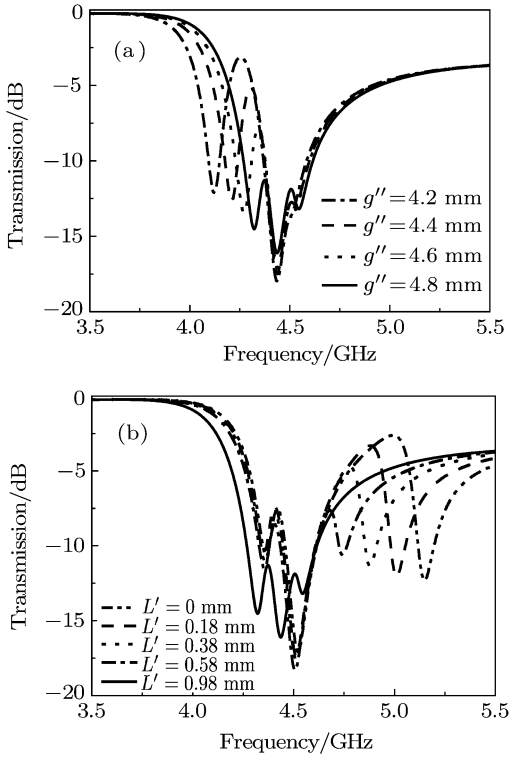


Fig. 6. The simulated transmission characteristic for Fig. 5(a). (a) The gap of the outer pair-SRR (g'') is changed when the dimensions of the other pair-SRRs are fixed. (b) The arm length of inner pair-SRR (L') is changed when the dimensions of the other pair-SRRs are fixed.

Additionally, the stability of negative permeability for the proposed SRRs in Fig. 5(a) has been discussed. Figure 7 shows that the dielectric loss tangent of the substrate, which supports the metallic SRRs, has great influence on the vibration of negative permeability. When the loss tangent of the substrate is zero, the variation of its electromagnetic parameters is very sharp and the MNG bandwidth for each SRR is too narrow to combine the three MNG frequency bands to design a wideband MNG material. However, if a substrate with a higher loss tangent is selected, the negative permeability vibration drops and keeps a higher stability without discontinuity, especially when the loss tangent is equal to 0.03. Therefore, a substrate of a little higher loss tangent, which has less variation in electromagnetic parameters, is more suitable for designing a wideband MNG material. On the other hand, the additional dialectic loss from the substrate of ahigh loss tangent must be taken into consideration, because it is of little use in the application when the dielectric loss is too high. Considering

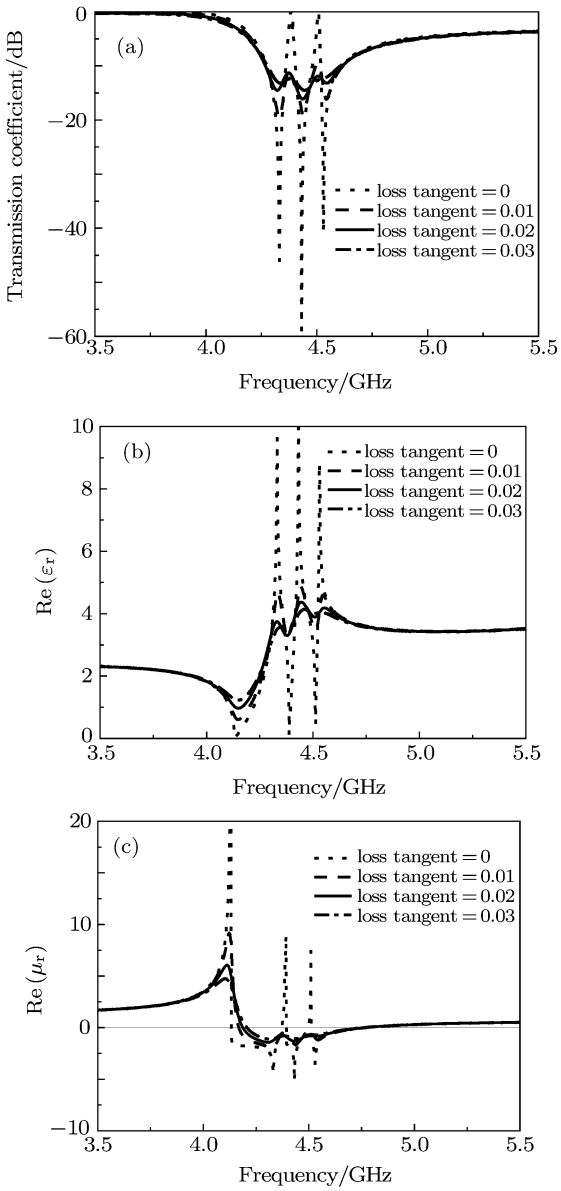


Fig. 7. Effect of the dielectric loss tangent on (a) transmission characteristics and the retrieved electromagnetic parameters; (b) effective permittivity, (c) effective permeability.

the above two factors, a substrate with a moderate dielectric loss tangent should be selected as a compromise on the basis of the engineering requirements in its practical application.

The resonant response of the above MNG material is measured using two coaxial probes connected to an AV3618 network analyser and a similar experimental program was been adopted in Refs. [23], [29], and [32]. First, we measure the transmission spectra in the free space, i.e., without the MNG material. The data are recorded for calibration and then the measurement with the above MNG materials inserted (Fig. 8) is repeated. The distance between the receiver and transmitter probes is kept fixed during the experiment. The measured results are also shown in Fig. 8, in which the positive transmission values are caused by the calibration technique and the lensing effect of the structures.[23] Verifying the effectiveness of the proposed evolution approach in Fig. 4, the measurement results lead to the conclusion that when the SRRs are added and arranged, this MNG material structure can achieve resonance frequency bandwidth expansion step by step within the tolerable experimental error.

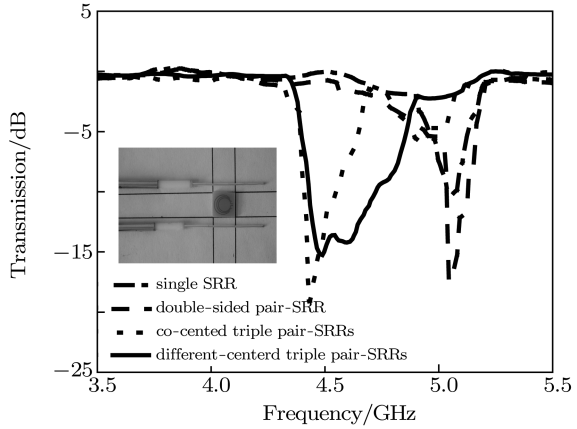


Fig. 8. Measured transmission data as a function of the frequency for different types of SRRs (the measured sample is in the middle of the two probes).

4. Conclusion

In summary, an effective approach to expand the bandwidth of a planar MNG material is proposed. The fractional bandwidth of the MNG material is expanded from 3.53% to 12.87% by adding SRRs and changing the relative positions step by step, according to the analysis of equivalent circuit models. The experiment verifies the effectiveness of the bandwidth-expanding methods at each step. For further investigation, we point out the possibility of further broadeninf the MNG bandwidth by employing more SRRs using this evolution method. It is also worthwhile mentioning that when more SRRs are added step by step to expand the MNG bandwidth, the length of the arm and the relative position of all these SRRs (including original SRRs and additional SRRs) needs to be accommodated, increasing the complexity of the design.

References

[1] Veselago V G 1968 *Sov. Phys. Usp.* **10** 509
[2] Zhang Y P, Zhao X P, Bao S and Luo C R 2010 *Acta Phys. Sin.* **59** 6078 (in Chinese)
[3] Sun Y Z, Ran L X, Peng L, Wang W G, Li T, Zhao X and Chen Q L 2009 *Chin. Phys.* B **18** 174
[4] Yang R, Xie Y J, Li X F, Jiang J, Wang Y Y and Wang R 2009 *Acta Phys. Sin.* **58** 901 (in Chinese)
[5] Xu F, Bai Y, Qiao L J, Zhao H J and Zhou J 2009 *Chin. Phys.* B **18** 1653
[6] Fan J and Cai G Y 2010 *Acta Phys. Sin.* **59** 6084 (in Chinese)
[7] Zhang H F, Cao D, Tao F, Yang X H, Wang Y, Yan X N and Bai L H 2010 *Chin. Phys.* B **19** 027701
[8] Xiang Y J, Wen S C and Tang K S 2006 *Acta Phys. Sin.* **55** 2714 (in Chinese)
[9] Pendry J B, Holden A J, Stewart W J and Youngs I 1996 *Phys. Rev. Lett.* **76** 4773
[10] Pendry J B, Holden A J, Robbins D J and Stewart W J 1999 *IEEE Trans. Microw. Theory Tech.* **47** 2075
[11] Baena J D, Marques R, Medina F and Martel J 2004 *Phys. Rev.* B **69** 014402
[12] Chen H, Ran L, Huangfu J, Zhang X, Chen K, Grzegorczyk T M and Kong J A 2004 *Phys. Rev.* E **70** 057605
[13] Wu B I, Wang W, Pacheco J, Chen X, Grzegorczyk T and Kong J A 2005 *Prog. Electromagn. Res.* **51** 295
[14] Enkrich C, Wegener M, Linden S, Burger S, Zschiedrich L, Schmidt F, Zhou J F, Koschny Th and Soukoulis C M 2005 *Phys. Rev. Lett.* **95** 20
[15] Ekmekci E and Turhan-Sayan G 2010 *Electron. Lett.* **46** 5
[16] Ekmekci E, Topalli K, Akin T and Turhan-Sayan G 2009 *Opt. Express* **17** 16046
[17] Lepetit T, Akmansoy É, Paté M and Ganne J P 2008 *Electron. Lett.* **44** 19
[18] Rudolph S M and Grbic A 2007 *J. Appl. Phys.* **102** 013904
[19] Rudolph S M and Grbic A 2008 *IEEE Trans. Antennas Propag.* **56** 2963
[20] Zharov A A, Shadrivov I V and Kivshar Y S 2003 *Phys. Rev. Lett.* **91** 037401
[21] *Ansoft High Frequency Structure Simulation* (HFSS) 2005 Ansoft Corp., ver. 10

[22] Smith D R, Jonah G, Jack J M, Willie J P and David S 2006 *J. Appl. Phys.* **100** 024507
[23] Alici K B, Bilotti F, Vegni L and Ozbay E 2007 *Appl. Phys. Lett.* **91** 071121
[24] Baena J D, Marqués R, Medina F and Martel J 2004 *Phys. Rev.* B **69** 014402
[25] Baena J D, Bonache J, Martín F, Sillero R M, Falcone F, Lopetegi T, Laso M A G, García–García J, Gil I, Portillo M F and Sorolla M 2005 *IEEE Trans. Microwave Theory Tech.* **53** 1451
[26] Smith D R, Vier D C, Koschny Th and Soukoulis C M 2005 *Phys. Rev.* E **71** 036617
[27] Koschny T, Markoš P, Smith D R and Soukoulis C M 2003 *Phys. Rev.* E **68** 065602(R)
[28] Gay-Balmaz P and Martina O J F 2002 *J. Appl. Phys.* **92** 5
[29] Bilotti F, Toscano A, Vegni L, Aydin K, Alici K B and Ozbay E 2007 *IEEE Trans. Microwave Theory Tech.* **55** 2865
[30] Wang J F, Qu S B, Xu Z, Ma H, Yang Y M and Gu C 2008 *IEEE Trans. Antennas Propag.* **56** 2018
[31] Tang M C, Xiao S Q, Deng T W, Wang D, Bai Y Y, Jin D P and Wang B Z 2011 *Acta Phys. Sin.* **60** 064101 (in Chinese)
[32] Bulu I, Caglayan H, Aydin K and Ozbay E 2005 *New J. Phys.* **7** 223